

NEAR-INFRARED SPECTROSCOPIC ANALYSIS OF ACID-TREATED ORGANO-CLAYS

JANA MADEJOVÁ*, HELENA PÁLKOVÁ, MARTIN PENTRÁK, AND PETER KOMADEL

Institute of Inorganic Chemistry, SAS, Dúbravská cesta 9, SK-845 36 Bratislava, Slovakia

Abstract—The potential use of near-infrared (NIR) spectroscopy as a characterization tool for organo-clays would be a great asset but little work has been done in this regard because the application of NIR to clay mineral studies is a relatively new phenomenon. The purpose of this study was to use NIR spectroscopy to investigate the effect of alkylammonium cations on the acid dissolution of a high-charge montmorillonite (SAz-1). Detailed analysis of the spectra of Li^+ , TMA^+ (tetramethylammonium), and HDTMA^+ (hexadecyltrimethylammonium) saturated SAz-1 montmorillonite in the NIR region was achieved by comparing the first overtone (2ν) and combination ($\nu+\delta$) bands of $X\text{H}$ groups ($X = \text{O}, \text{C}$) with the fundamental stretching (ν) and bending (δ) vibrations observed in the mid-infrared (MIR) region. Comprehensive analysis of the vibrational modes of CH_3-N , CH_3-C , and $-\text{CH}_2-\text{C}$ groups of TMA^+ and HDTMA^+ cations detected in the MIR and NIR regions was also performed. Both MIR and NIR spectra demonstrated that exchange of Li^+ by TMA^+ only slightly improved the resistance of SAz-1 layers to dissolution in 6 M HCl at 80°C, while exchange by the larger HDTMA^+ cations almost completely protected the montmorillonite layers from acid attack. Use of NIR spectra in reaching these conclusions was crucial. Only in the NIR region could the creation of SiOH groups be monitored, which is an important indicator of the acidification of the montmorillonite surface. The OH-overtone region in the spectra of Li-SAz-1 and TMA-SAz-1 revealed that the SiOH band near 7315 cm^{-1} increases in intensity with enhanced acid treatment. In contrast, no SiOH groups were identified in the NIR spectra of HDTMA-SAz-1 treated in HCl, indicating that HDTMA^+ completely covers the inner and outer surfaces of the montmorillonite and hinders access of protons to the $\text{Si}-\text{O}^-$ bonds created upon acid treatment.

Key Words—Acid Treatment, Alkylammonium Cations, NIR Spectroscopy, Organo-clays, Structural Modifications.

INTRODUCTION

The technique of near infrared (NIR) spectroscopy, covering the spectral range $12,000$ – 4000 cm^{-1} , is undergoing dynamic development and spreading into many areas of science and technology (Bokobza, 1998; Williams and Norris, 1987; Workman and Weyer, 2008). The interest in the method arises from improvements in NIR spectrometers, the development of chemometric methods, and the introduction of optical fibers allowing transfer of NIR energy and information. Among the advantages offered by NIR spectroscopy, speed, simplicity of sample preparation, and the non-destructive nature of the technique are the most attractive. The method appears well suited to on-line quality control in various branches of industry (Williams and Norris, 1987; Prüfer and Mamma, 1995), for analysis of the minerals on Earth (Hunt and Salisbury, 1970) and Mars (Bishop *et al.*, 2004; Bishop *et al.*, 2008a), or for exploration of soils (Malley *et al.*, 2002) and clay deposits (Dill *et al.*, 2005) by portable IR analyzers. NIR spectroscopy has also been used for clay-mineral characterization (Petit *et*

al., 1999; Madejová and Komadel, 2001; Gates *et al.*, 2002; Frost *et al.*, 2002; Petit, 2005; Gates, 2005; Gionis *et al.*, 2007; Bishop *et al.*, 2008b), including investigation of structural changes occurring upon heating of smectites saturated with small exchangeable cations (Madejová *et al.*, 2000; Petit *et al.*, 2002; Pálková *et al.*, 2003; Madejová, 2005). Recently, NIR spectroscopy was used successfully to monitor the acid dissolution of Fe-bentonite (Madejová *et al.*, 2007) and different kinds of naturally occurring clay minerals, showing the effects of the structure, chemical composition, and the availability of the interlayer space on the extent of dissolution (Madejová *et al.*, 2009).

One of the most frequently used modifications of clay minerals is the intercalation of organic species into their interlayers (Yariv and Cross, 2001; Theng, 1974). Of the spectroscopic techniques, infrared spectroscopy in the MIR region (4000 – 400 cm^{-1}) is often used to characterize the interactions of organic substances with clay minerals (Breen *et al.*, 1997; Yariv, 2001; Zhu *et al.*, 2005; Frost *et al.*, 2008; Önal and Sankaya, 2008). The inorganic exchangeable cations in smectites are frequently replaced by quaternary alkylammonium cations to modify their properties and to change the surface of smectite to make it more hydrophobic (Boyd *et al.*, 1988; Stevens and Anderson, 1996). The presence of alkylammonium cations also affects the rate of dissolution of smectites in acids

* E-mail address of corresponding author:
jana.madejova@savba.sk
DOI: 10.1346/CCMN.2009.0570311

(Breen and Watson, 1998; Moronta *et al.*, 2002). The MIR spectra clearly show that the long-chain alkylammonium cations restrict access of protons to the layers so the extent of acid attack is reduced (Breen *et al.*, 1997). A few studies have reported on the use of NIR spectroscopy in adsorption studies of organic molecules on smectites (Zhou *et al.*, 2008) and none, to our knowledge, on the NIR study of acid-treated organo-clays.

This study revealed the potential of NIR spectroscopy in investigations of organo-clays. The NIR spectra of two alkylammonium derivatives of montmorillonite were analyzed in detail and the influence of the size of alkylammonium cations on the dissolution rate of organo-clays in HCl was determined. Results revealed that NIR spectra can be used successfully to characterize organic molecules adsorbed on Cheto montmorillonite and to identify structural changes occurring upon chemical treatment of organo-clays.

EXPERIMENTAL

Materials

The fine fraction of bentonite from Cheto (SAz-1), Arizona, USA, obtained from the Source Clays Repository of The Clay Minerals Society was used in this study. The bentonite was suspended in distilled water, Li-saturated by repeated treatment with 1 M LiCl, and the <2 µm fraction collected. The suspension was washed free of excess salts, dried at 60°C, and ground to pass a 0.2 mm sieve in order to prepare the Li-SAaz-1 sample. Organo-clays were prepared by cation exchange reactions of the Li-SAaz-1 with tetramethylammonium (TMA^+) chloride or hexadecyltrimethylammonium (HDTMA^+) bromide. Alkylammonium salts were dissolved in a 50:50 (by volume) mixture of distilled water and ethanol. The amount of organic cation used for exchange was three times (HDTMA^+) and seven times (TMA^+), respectively, the cation exchange capacity (CEC) of the montmorillonite. The suspension of montmorillonite and organic solution was stirred for 16 h at ~60°C. The excess alkylammonium salts were removed by repeated washing with a mixture of ethanol and distilled water. The dried samples are referred to as HDTMA-SAaz-1 and TMA-SAaz-1.

The Li-, TMA-, and HDTMA-SAaz-1 samples were further dissolved in 6 M HCl at 80°C for 2 and 6 h. After the acid treatments, the samples were filtered, washed with de-ionized water, centrifuged, dried, and ground as described above.

FTIR spectroscopy

The IR spectra were obtained using a Nicolet Magna 750 Fourier transform infrared spectrometer. For the spectra in the NIR region, a PbSe detector, CaF_2 beam splitter, and the DRIFT technique were used. For the MIR region, a DTGS detector, a KBr beam splitter, and the KBr pressed-disk technique (1 mg of sample and

200 mg of KBr) were used. For each sample, 128 scans with a resolution of 4 cm^{-1} were recorded.

Spectra manipulations were performed using the OMNIC software package (Nicolet Instruments Corp.). The accuracy in determining the positions of the absorption bands was $\pm 1 \text{ cm}^{-1}$. In order to find the location of a peak appearing in the spectrum as a shoulder, a Fourier Self Deconvolution (FSD) routine and second-derivative operation (with OMNIC default parameters) were used. The difference between the wavenumber values obtained did not exceed 2 cm^{-1} . The assignment of the absorption bands of natural clay minerals in the MIR region follows Farmer (1974). The assignments of the bands in the NIR region together with relevant references are given in the Results and Discussion section below.

RESULTS AND DISCUSSION

Identification of MIR bands characteristic of TMA^+ and HDTMA^+ cations

The absorption bands associated with OH, NH, and CH functional groups dominate in the spectra of organo-clays taken in the NIR region. These absorptions arise from overtones of fundamental stretching vibrations or combinations involving stretching (ν) and bending (δ) modes of $X\text{H}$ ($X = \text{O}, \text{N}, \text{C}$) groups. Overtone bands occur when a fundamental vibrational mode is excited with two or more quanta, whereas combination bands represent the coupling between different vibrational modes. A NIR spectrum, however, cannot be interpreted in as straightforward a manner as a MIR spectrum. While the MIR spectra exhibit well defined peaks related to fundamental modes, the NIR spectra often contain broad bands resulting from several overlapping peaks. In addition, the presence of Fermi resonances can also increase the complexity of the NIR spectra (Bokobza, 1998). For identification of individual bands related to CH overtones and combination modes of CH_3 and CH_2 groups present in the NIR spectra of TMA-SAaz-1 and HDTMA-SAaz-1, the MIR spectra of Li-SAaz-1 and both organo-clays (Figure 1) were analyzed.

The characteristic bands assigned to stretching and bending vibrations of O-H and Si-O groups of Li-SAaz-1 montmorillonite occur in the 4000–3400 cm^{-1} and 1200–400 cm^{-1} regions (Figure 1a). The OH stretching band appears at 3620 cm^{-1} , while the AlAlOH and AlMgOH bending bands are observed at 916 cm^{-1} and 843 cm^{-1} , respectively. The Si-O stretching mode is at 1033 cm^{-1} , and the Si-O-Al and Si-O-Si bending vibrations absorb at 519 cm^{-1} and 465 cm^{-1} , respectively. Exchange of inorganic Li^+ cations with TMA^+ and HDTMA^+ modified the shape of the MIR spectra of organo-clays (Figures 1b,c). In addition to OH and Si-O vibrations, the absorption bands related to CH-stretching and -bending vibrations became visible. The MIR spectra of compounds containing TMA^+ and HDTMA^+

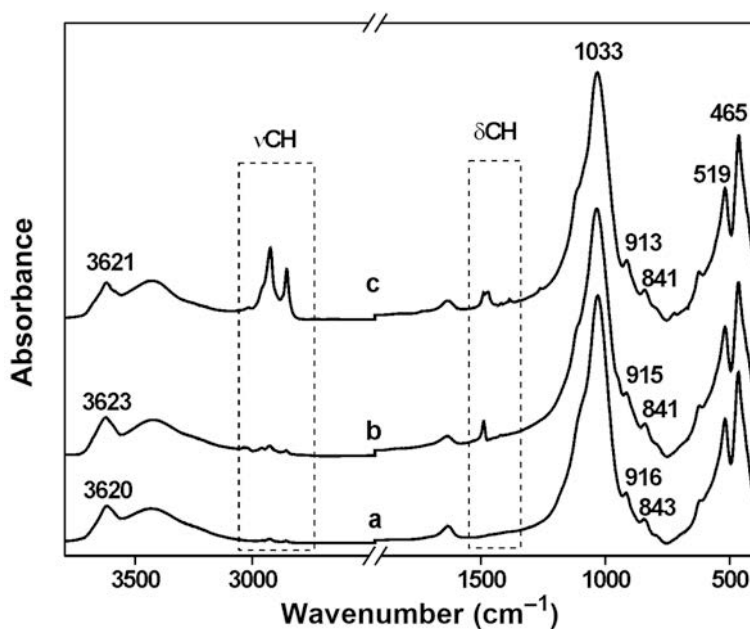


Figure 1. MIR spectra of Li-SAz-1 (a), TMA-SAz-1 (b), and HDTMA-SAz-1 (c).

cations should show asymmetric (ν_{as}) and symmetric (ν_s) stretching (at ~ 3050 – 2800 cm^{-1}), asymmetric (δ_{as}) and symmetric (δ_s) bending (at ~ 1500 – 1300 cm^{-1}), and rocking (at ~ 1280 – 1000 cm^{-1}) vibrations of CH_3 and CH_2 groups together with νCN (~ 950 , 750 cm^{-1}) and δCNC ($\sim 450\text{ cm}^{-1}$) modes (Zeegers-Huyskens and Bator, 1996). However, only CH_3 and CH_2 stretching and bending bands were clearly visible in the MIR spectra of organo-clays, the other absorptions occurring below 1100 cm^{-1} were overlapped by stronger Si-O bands of the montmorillonite (Figure 1).

Comparing the CH-stretching and -bending regions in the spectra of TMA-SAz-1, HDTMA-SAz-1, and of the salts used for their preparation, *i.e.* TMA-Cl and HDTMA-Br, revealed (Figure 2) that two CH stretching bands, $\nu_{as}\text{CH}_3$ and $\nu_s\text{CH}_3$, are expected to be present in the spectrum of TMA-Cl. However, Figure 2A,a shows instead a complex pattern for TMA-Cl with several overlapping bands and shoulders. Similar to other tetraalkylammonium ions (Zeegers-Huyskens and Bator, 1996), more bands in Figure 2A resulted from a Fermi resonance interaction with a δCH_3 level. The most pronounced absorption near 3015 cm^{-1} corresponds to $\nu_{as}\text{CH}_3$ vibration while the bands near 2960 cm^{-1} and 2920 cm^{-1} have been reported for $\nu_s\text{CH}_3$ (Zeegers-Huyskens and Bator, 1996). The intense band at 1488 cm^{-1} is assigned to the $\delta_{as}\text{CH}_3$ vibration while the $\delta_s\text{CH}_3$ mode gives an absorption band with peaks at 1404 cm^{-1} and 1399 cm^{-1} (Figure 2B,a). Less intense and more diffuse CH₃ bands in the spectrum of TMA-SAz-1 (Figures 2A,b and 2B,b) indicate less organic phase in the organo-clay than in TMA-Cl. A shift of the $\nu_{as}\text{CH}_3$ band to higher wavenumber ($\sim 3030\text{ cm}^{-1}$) reflects the

interaction of the $(\text{CH}_3)_4\text{N}^+$ cations with the montmorillonite layers. Both the positions and assignments of the CH_3 bands observed in the MIR spectrum of TMA-SAz-1 are listed in Table 1.

Replacement of one methyl group in the $(\text{CH}_3)_4\text{N}^+$ cation with a longer alkyl chain, as in the $\text{CH}_3(\text{CH}_2)_{15}\text{N}^+(\text{CH}_3)_3$ cation, significantly modified the shape of the spectra of HDMA-Br and HDTMA-SAz-1 (Figures 2C,D). The $\text{CH}_3\text{-N}$, $\text{CH}_3\text{-C}$, $\text{CH}_2\text{-N}$, and $\text{CH}_2\text{-C}$ groups should be considered for analysis of the vibration modes in the spectra of HDTMA⁺. However, resolving unambiguously the absorption bands of individual groups in the MIR region is quite difficult due to overlap. The spectrum of HDTMA-Br shows a complex band in the 3050 – 3000 cm^{-1} region with two absorptions at 3030 cm^{-1} and 3017 cm^{-1} corresponding to the $\nu_{as}\text{CH}_3\text{-N}$ vibrations (Figure 2C,a). Based on comparison with the TMA-Cl spectrum, the absorption at 2958 cm^{-1} should be due to $\nu_s\text{CH}_3\text{-N}$ vibrations, while the 2943 cm^{-1} band may be related to $\nu_{as}\text{CH}_3\text{-C}$. The assignment of the bands at 2918 cm^{-1} and 2850 cm^{-1} is unambiguous; these two strong bands originate from $\nu_{as}\text{CH}_2\text{-C}$ and $\nu_s\text{CH}_2\text{-C}$ modes, respectively. The weak band at 2871 cm^{-1} corresponds to $\nu_s\text{CH}_3\text{-C}$. The C-H bending region of HDTMA-Br revealed several bands (Figure 2D,a). The $\delta_{as}\text{CH}_3\text{-N}$ vibrations absorb at 1487 cm^{-1} , while the bands at 1473 cm^{-1} and 1463 cm^{-1} correspond to asymmetric bending vibrations of $\text{CH}_2\text{-C}$ groups. The weak bands below 1430 cm^{-1} might be related to $\delta_s\text{CH}_3\text{-N}$ and/or $\delta_s\text{CH}_2\text{-C}$.

In comparison with HDTMA-Br, the MIR spectrum of HDTMA-SAz-1 contained less intense and fewer resolved bands corresponding to C-H vibrations (Figures 2C,b and 2D,b). Only $\nu_{as}\text{CH}_2\text{-C}$ and $\nu_s\text{CH}_2\text{-C}$ vibrations

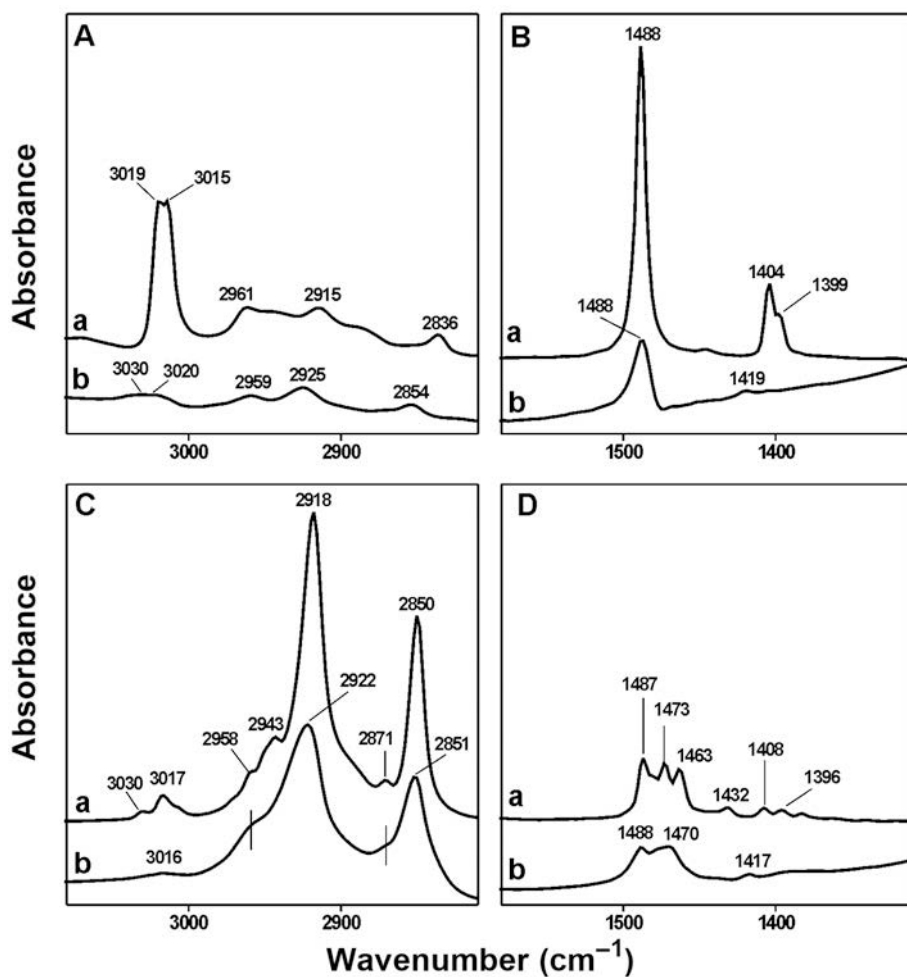


Figure 2. CH stretching (A) and bending (B) regions of TMA-Cl (a) and TMA-SAz-1 (b), and CH stretching (C) and bending (D) regions of HDTMA-Br (a) and HDTMA-SAz-1 (b).

absorbing at 2922 cm^{-1} and 2851 cm^{-1} are clearly recognized; other C-H stretching modes appear as broad shoulders or weak inflections. Using the FSD routine, the positions for $\nu_{as}\text{CH}_3\text{-N}$ and $\nu_s\text{CH}_3\text{-C}$ were identified at 3016 cm^{-1} and 2872 cm^{-1} , respectively. A broad shoulder near 2960 cm^{-1} is due to $\nu_s\text{CH}_3\text{-N}$ overlapping a band near 2950 cm^{-1} related to $\nu_{as}\text{CH}_3\text{-C}$. Corresponding deformation modes of CH_3 and CH_2 groups were observed in the $1500\text{--}1400\text{ cm}^{-1}$ region. The $\delta_{as}\text{CH}_3\text{-N}$ vibrations give rise to a band at 1488 cm^{-1} , while a broad band near 1470 cm^{-1} is caused by vibrations of $\delta_{as}\text{CH}_2\text{-C}$ groups. A weak band near 1417 cm^{-1} may be attributed to a symmetric C-H deformation mode (Table 2).

Identification of NIR bands characteristic of Li-SAz-1, TMA-SAz-1, and HDTMA-SAz-1

The NIR spectra of Li-, TMA-, and HDTMA-SAz-1 montmorillonites (Figure 3) revealed bands in the $8000\text{--}4000\text{ cm}^{-1}$ region, which derive from the first overtone ($2\nu\text{OH}$ and $2\nu\text{CH}$) and combination ($(\nu+\delta)\text{OH}$

and $(\nu+\delta)\text{CH}$) modes of fundamental stretching and bending vibrations. As a result of the anharmonic character of vibrations, the positions of the bands are lower than the theoretical values calculated from the wavenumber values of the corresponding MIR bands (Bokobza, 1998; Balan *et al.*, 2007; Workman and Weyer, 2008). Petit *et al.* (2004) showed that the location of the first OH-overtone band in NIR spectra of various clay minerals is $\sim 170\text{ cm}^{-1}$ less than the value calculated from the νOH positions. The calculated average value of the anharmonicity constant was -86.5 cm^{-1} . This parameter is unique for each bond because it depends on the nature and environment (e.g. formation of hydrogen bonds, intermolecular interactions, etc.) of vibrating groups. Balan *et al.* (2007) reported that the anharmonicity constant increases from -93 to -300 cm^{-1} when the OH-stretching frequency decreases from 3700 to 2900 cm^{-1} , suggesting that the anharmonicity of the OH bond increases with the strength of the H-bonding between the OH group and the surrounding oxygens. Thus, substantial variability in

Table 1. Positions and assignments of the CH_3 bands observed in the NIR and MIR spectra of TMA-SAZ-1 and the theoretically calculated values of overtone and combination modes.

Observed position (cm^{-1})	Assignment	Calculated value ⁺ (cm^{-1})
6048	$2\nu_{\text{as}}$	6060; (2×3030)
6014	$2\nu_{\text{as}}$	6040; (2×3020)
5920	$\nu_{\text{as}} + \nu_s$	5945; ($3020 + 2925$)
5880	$2\nu_s$	5918; (2×2959)
5825	$2\nu_s$	5850; (2×2925)
4471*	$(\nu + \delta)_{\text{as}}$	4518; ($3030 + 1488$)
4447	$(\nu + \delta)_{\text{as}}$	4508; ($3020 + 1488$)
4324	$\nu_s + \delta_s$	4378; ($2959 + 1419$)
4268*	$\nu_s + \delta_s^{\#}$	4344; ($2925 + 1419$)
4203	$\nu_{\text{as}} + \text{r}^{\#}$	4327; ($3030 + 1297$)
4105	$\nu_{\text{as}} + \text{r}^{\#}$	4222; ($2925 + 1297$)
3030	ν_{as}	
3020*	ν_{as}	
2959	ν_s	
2925	ν_s	
1488	δ_{as}	
1419	δ_s	

⁺ value calculated from the observed fundamental vibrations

* wavenumber value obtained by FSD and/or 2nd derivative
r [#] CH_3 rocking vibrations observed only in the spectrum of $(\text{CH}_3)_4\text{N-Cl}$

the differences between the observed and calculated OH- and CH-band positions can be expected in the organo-clays studied.

The NIR spectrum of Li-SAZ-1 (Figure 3a) shows a broad, complex band at 7060 cm^{-1} containing overlapping contributions of the first overtone of structural

Table 2. Positions and assignments of the CH_3 and CH_2 bands observed in NIR and MIR spectra of HDTMA-SAZ-1 and the theoretically calculated values of overtone and combination modes.

Observed (cm^{-1})	Assignment	Calculated value ⁺ (cm^{-1})
6039	$2\nu_{\text{as}}\text{CH}_3\text{-N}$	6060; ($2 \times 3030^{\#}$)
5998	$2\nu_s\text{CH}_3\text{-N}$	6032; (2×3016)
5911*	$2\nu_s\text{CH}_3\text{-N}$	5920; (2×2960)
5864*	$2\nu_{\text{as}}\text{CH}_3\text{-C}$	5886; ($2 \times 2943^{\#}$)
5785	$2\nu_{\text{as}}\text{CH}_2\text{-C}$	5844; (2×2922)
5688	$2\nu_s\text{CH}_3\text{-C}$	5744; ($2 \times 2871^{\#}$)
	$2\nu_s\text{CH}_2\text{-C}$	5702; (2×2851)
4463	$(\nu_{\text{as}} + \delta_{\text{as}})\text{CH}_3\text{-N}$	4518; ($3030 + 1488$)
4440	$(\nu_{\text{as}} + \delta_{\text{as}})\text{CH}_3\text{-N}$	4504; ($3016 + 1488$)
4330	$(\nu_{\text{as}} + \delta_{\text{as}})\text{CH}_2\text{-C}$	4392; ($2922 + 1470$)
4255	$(\nu_s + \delta_s)\text{CH}_2\text{-C}$	4268; ($2851 + 1417$)
4156		complex band
3016	$\nu_{\text{as}}\text{CH}_3\text{-N}$	
2960*	$\nu_s\text{CH}_3\text{-N}, \nu_{\text{as}}\text{CH}_3\text{-C}$	see text
2922	$\nu_{\text{as}}\text{CH}_2\text{-C}$	
2872*	$\nu_s\text{CH}_3\text{-C}$	
2851	$\nu_s\text{CH}_2\text{-C}$	
1488	$\delta_{\text{as}}\text{CH}_3\text{-N}$	
1470	$\delta_{\text{as}}\text{CH}_2\text{-C}$	
1417	$\delta_s\text{CH}_2\text{-C}, \delta_s\text{CH}_3\text{-N}$	

⁺ value calculated from the observed fundamental vibrations

* wavenumber value obtained by FSD and/or 2nd derivative

vibrational band observed only in the spectrum of HDTMA-Br

OH groups ($2\nu\text{OH}$) and the first overtone of stretching vibrations of H_2O molecules. Considering the anharmonicity, the corresponding asymmetric stretching vibra-

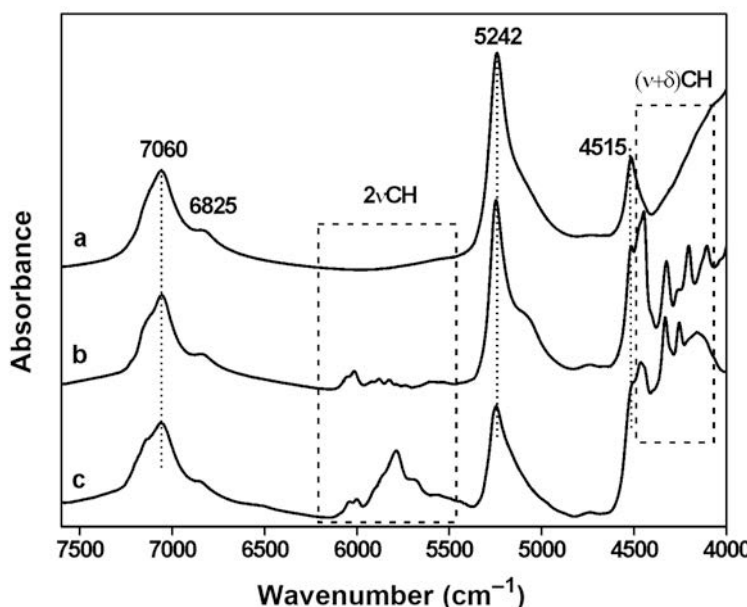


Figure 3. NIR spectra of Li-SAZ-1 (a), TMA-SAZ-1 (b), and HDTMA-SAZ-1 (c)

tion ($\nu_{as}\text{H}_2\text{O}$) should appear in the $\sim 3630\text{--}3610\text{ cm}^{-1}$ region. The shoulder near 6825 cm^{-1} is due to the first overtone of symmetric stretching vibrations of water molecules involved in strong hydrogen bonds ($\nu_s\text{H}_2\text{O} = \sim 3430\text{ cm}^{-1}$). Detailed analysis of the spectral features attributed to water molecules in both the MIR and NIR regions was given by Bishop *et al.* (1994). The intense band near 5242 cm^{-1} is due to $(\nu+\delta)\text{H}_2\text{O}$ while the band at 4515 cm^{-1} is attributed to a combination mode of structural OH groups (Madejová and Komadel, 2001). Displacement of hydrated Li^+ with TMA^+ and HDTMA^+ cations in SAz-1 affects the shape of the NIR spectra. In addition to the $2\nu\text{OH}$ and $(\nu+\delta)\text{OH}$ bands of montmorillonite, the C-H overtone and combination bands appear in the $6100\text{--}5500\text{ cm}^{-1}$ and $4500\text{--}4000\text{ cm}^{-1}$ regions, respectively (Figure 3b,c). No detailed analysis of the NIR spectra of montmorillonites saturated with alkylammonium cations is available in the literature. Thus, the assignment of the C-H overtones and combination modes given in Tables 1 and 2 is based on the interpretations reported for other alkylammonium salts (Zeegers-Huyskens and Bator, 1996) and on the theoretically calculated values of overtones and combination modes using bands observed in the MIR region.

Precise assignment of the vibrational modes of CH overtone and combination regions of the two organoclays (Figure 4) is difficult because the number of observed bands is significantly greater than predicted from the MIR spectra (Figure 2). The overtone and

combination bands may correspond to several possible combinations of C-H fundamental vibrations which are not clearly resolved in the MIR spectra of organo-clays but are visible in the MIR spectra of TMA- and HDTMA-salts. Moreover, distortion of the symmetry of alkylammonium cations may lead to splitting of the C-H overtone and combination bands. Therefore some bands were assigned to the same vibrational modes (Tables 1, 2). Similar doublets were also reported for other tetraalkylammonium ions (Zeegers-Huyskens and Bator, 1996).

Both the wavenumber values of the CH_3 and CH_2 fundamentals and the anharmonic character of vibrations must be taken into account to find the explanation of the bands present in the spectra shown in Figure 4. Due to the anharmonicity factor, the wavenumber positions of the observed bands should be less than the calculated values. The absorption bands observed in the $6100\text{--}5500\text{ cm}^{-1}$ region of the TMA-SAz-1 are assigned to two $2\nu_{as}\text{CH}_3$, two $2\nu_s\text{CH}_3$, and one combination $(\nu_{as}+\nu_s)\text{CH}_3$ vibrations (Figure 4A,a; Table 1). The clearly resolved band at 4515 cm^{-1} is due to the combination mode of the structural OH groups. Several strong bands appear in the $4500\text{--}4000\text{ cm}^{-1}$ region of TMA-SAz-1 (Figure 4B,a). Some correspond to combination modes of stretching and bending CH_3 vibrations present in the MIR spectrum. However, the rocking CH_3 vibration must be considered to find the possible combination for the bands at

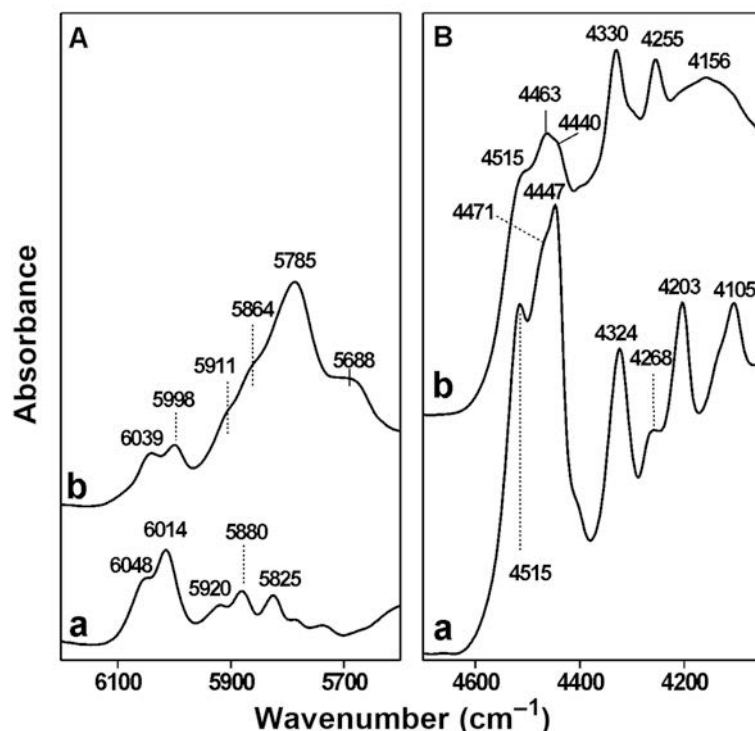


Figure 4. CH overtone (A) and combination (B) regions of TMA-SAz-1 (a) and HDTMA-SAz-1 (b).

4203 cm^{-1} and 4105 cm^{-1} (Table 1). No such band can be found in the MIR spectrum of TMA-SAz-1; however, a rocking CH_3 vibration at 1297 cm^{-1} (not shown in Figure 2) was identified in the spectrum of TMA-Cl.

The CH overtone and combination region of the HDTMA-SAz-1 sample (Figure 4b; Table 2) indicates that replacement of one methyl group in $(\text{CH}_3)_4\text{N}^+$ with a longer alkyl chain, $(\text{CH}_3)_3\text{N}^+(\text{CH}_2)_{15}\text{CH}_3$, made the shape of the NIR spectrum even more complex. The first CH overtones of $\text{CH}_3\text{-N}$ groups appeared in the 6100–5900 cm^{-1} region and the $2\nu_{\text{as}}\text{CH}_2\text{-C}$ and $2\nu_s\text{CH}_2\text{-C}$ bands were present at 5785 cm^{-1} and 5688 cm^{-1} , respectively. The broad shoulder near 5688 cm^{-1} also involves the contribution of $2\nu_s\text{CH}_3\text{-C}$ vibrations. The combination region revealed a shoulder near 4515 cm^{-1} due to $(\nu+\delta)\text{OH}$. The bands at 4463 cm^{-1} and 4440 cm^{-1} are attributed to combination modes of $\text{CH}_3\text{-N}$ groups, while the bands in the 4400–4000 cm^{-1} range should be related to combination vibrations of $\text{CH}_2\text{-C}$ groups (Table 2).

Dissolution of organo-clays in HCl

Dissolution of smectites in inorganic acids can lead to significant degradation of their structure. Protons penetrate into the layers and attack the OH groups, starting with those which are close to the isomorphic substitution sites. The resulting dehydroxylation is related to successive release of the octahedral atoms. At the same time, the transformation of the tetrahedral

sheets to a three-dimensional Si-O framework proceeds (Tkáč *et al.*, 1994; Komadel *et al.*, 1996; Komadel and Madejová, 2006). The alteration of the structure of the Li-SAz-1, TMA-SAz-1, and HDTMA-SAz-1 montmorillonites treated with 6 M HCl at 80°C was first studied by MIR spectroscopy (Figure 5). As an indicator of the extent of the decomposition of the smectite structure, the absorption band at 1033 cm^{-1} , corresponding to stretching vibrations of the Si-O groups, was chosen. The spectra of HCl-treated Li-SAz-1 show a gradual shift of the Si-O band from 1033 cm^{-1} , the characteristic position of tetrahedra arranged in the sheets of montmorillonite layers, to 1097 cm^{-1} , *i.e.* the position of the Si-O stretching vibrations of the reaction product – amorphous silica with a three-dimensional framework (Figure 5A). Two components in the spectrum of the sample treated for 2 h reflect the presence of both the smectite with layered arrangement (1044 cm^{-1}) and amorphous silica with three-dimensional framework (1082 cm^{-1}). The position of the Si-O band after 6 h of dissolution (1097 cm^{-1}) reflects complete decomposition of the Li-SAz-1 montmorillonite structure.

The stability of smectites in acids is changed if Li^+ cations are replaced by alkylammonium ions (Figure 5B,C). Dissolution of TMA-SAz-1 and HDTMA-SAz-1 proceeds much more slowly. After 2 h, the Si-O band in the spectra of both samples remained at a similar position as in the untreated samples, demonstrating minimal alteration of the smectitic layers. The

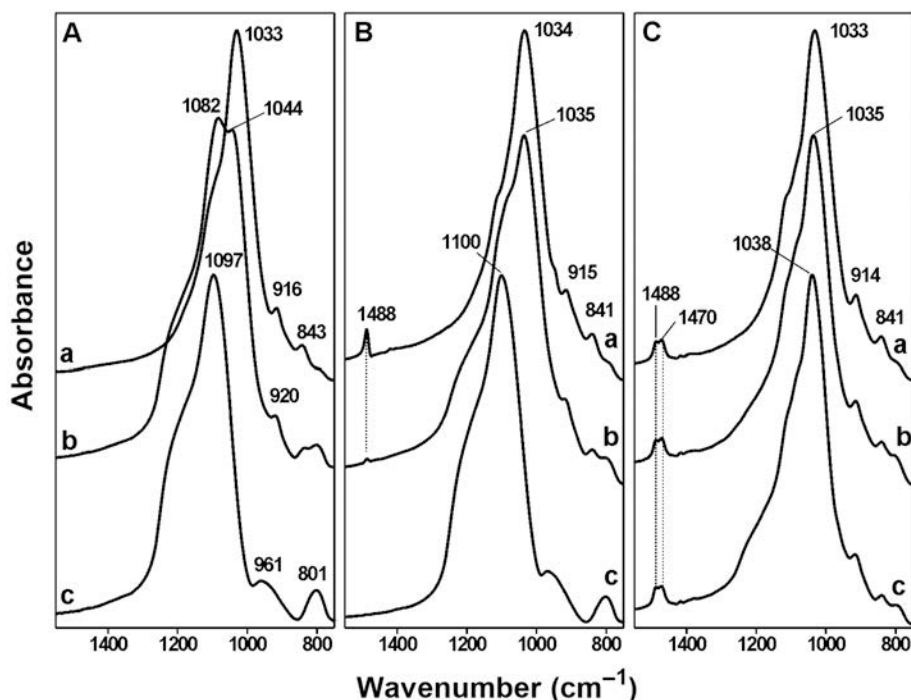


Figure 5. MIR spectra of Li-SAz-1 (A), TMA-SAz-1 (B), and HDTMA-SAz-1 (C): untreated (a), treated in 6 M HCl at 80°C for 2 h (b), and 6 h (c).

almost complete disappearance of the 1488 cm^{-1} band implies that TMA^+ cations were fully replaced by protons. On the other hand, no changes in the CH bending region were visible for HDTMA-SA_z-1 treated for 2 or 6 h (Figure 5C,b, 5C,c). Significant differences were seen between the spectra of TMA-SA_z-1 and HDTMA-SA_z-1 treated for 6 h. While the position of the Si-O band of TMA-SA_z-1 at 1100 cm^{-1} indicates the presence of only amorphous silica, just a slight change in the Si-O band position (compared to the spectrum of the untreated sample) was found for HDTMA-SA_z-1. Modification of the HDTMA-SA_z-1 structure after 6 h of treatment in 6 M HCl at 80°C was only minor,

confirming that long-chain alkylammonium cations (HDTMA^+) are more resistant to displacement by H^+ than cations with short chains, *i.e.* TMA^+ .

Dissolution of smectites in HCl is related to gradual dehydroxylation and acidification of the surface and thus this process can be effectively followed by NIR spectroscopy (Pálková *et al.*, 2003; Madejová *et al.*, 2009). The NIR spectra of acid-treated Li-SA_z-1, TMA-SA_z-1, and HDTMA-SA_z-1 montmorillonites were compared (Figure 6) and details of the first CH overtone ($6150\text{--}5650\text{ cm}^{-1}$) and CH combination ($4650\text{--}4050\text{ cm}^{-1}$) regions of both organo-clays were also examined (Figure 7). The spectrum of untreated Li-

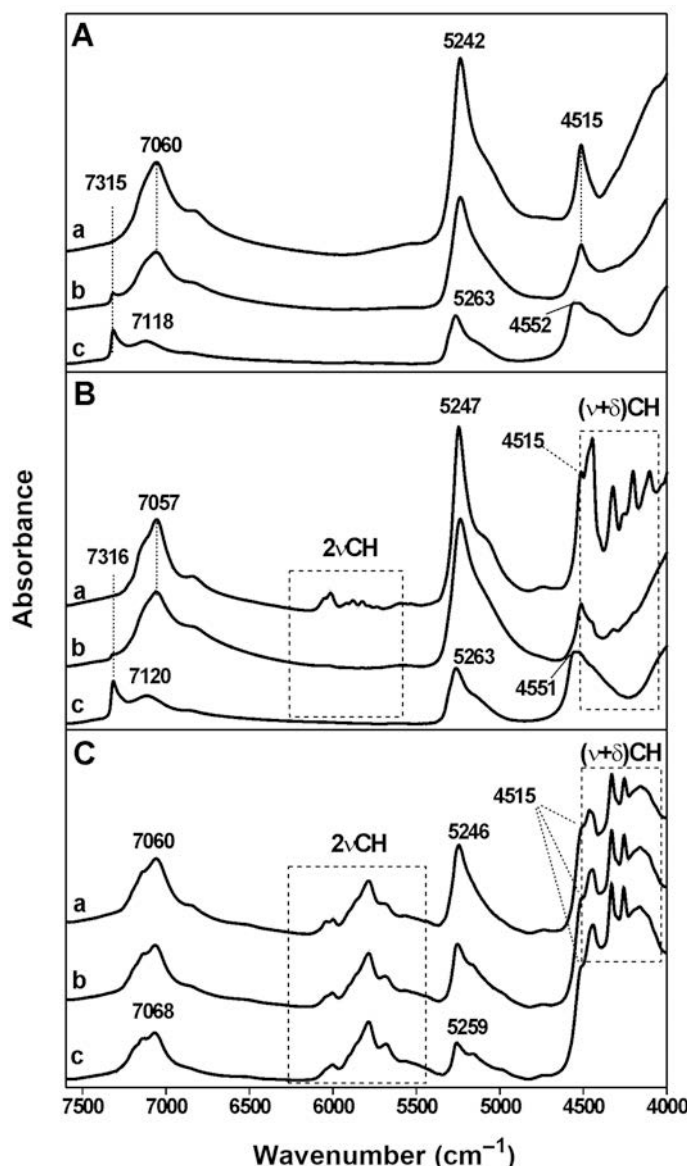


Figure 6. NIR spectra of Li-SA_z-1 (A), TMA-SA_z-1 (B), and HDTMA-SA_z-1 (C): untreated (a), treated in 6 M HCl at 80°C for 2 h (b), and 6 h (c).

SAz-1 contained a complex band related to $2\nu\text{OH}$ and $2\nu\text{H}_2\text{O}$ at 7060 cm^{-1} , $(\nu+\delta)\text{H}_2\text{O}$ at 5242 cm^{-1} , and $(\nu+\delta)\text{OH}$ at 4515 cm^{-1} . The OH overtone region of Li-SAz-1 treated with 6 M HCl for 2 h at 80°C (Figure 6A,b) revealed a decrease in the intensity of the band at 7060 cm^{-1} proving a release of OH groups and/or of the central atoms from the octahedral sheets. Moreover, the appearance of a new band at 7315 cm^{-1} assigned to the first SiOH overtone (Pálková *et al.*, 2003) confirmed the acidification of the Li-SAz-1 surface. Partial dehydroxylation of Li-SAz-1 after 2 h of dissolution in HCl is also reflected in the decreased intensity of the combination band at 4515 cm^{-1} . The lesser intensity of the $(\nu+\delta)\text{H}_2\text{O}$ band at 5242 cm^{-1} suggests fewer water molecules in the sample. Destruction of the smectite layers resulted in a smaller amount of exchangeable cation and, consequently, the amount of water adsorbed decreased.

The increased intensity of the $2\nu\text{SiOH}$ band (7315 cm^{-1}), and the reduced intensity and shift in

position of the overtone band from 7060 cm^{-1} to 7118 cm^{-1} , together with the appearance of the $(\nu+\delta)\text{SiOH}$ band at 4552 cm^{-1} , confirmed that 6 h of dissolution of Li-SAz-1 resulted in the creation of protonated amorphous silica. Concurrently, the $(\nu+\delta)\text{H}_2\text{O}$ band, the intensity of which decreased significantly in comparison with that of the untreated Li-SAz-1, shifted from 5242 cm^{-1} to 5263 cm^{-1} (Figure 6A,c). An upward shift of the $(\nu+\delta)\text{H}_2\text{O}$ band provides evidence that H_2O molecules adsorbed on the surfaces of destroyed layers and/or amorphous silica are less hydrogen bonded than those in the untreated clays. A more detailed discussion of the changes in the $(\nu+\delta)\text{H}_2\text{O}$ region was given by Madejová *et al.* (2009).

Comparing the NIR spectra of samples Li-SAz-1 and TMA-SAz-1 before and after HCl dissolution for 2 h (spectra b in Figure 6A,B) found that exchanging Li^+ with TMA^+ reduces the extent of alteration of SAz-1 by acid dissolution. The $2\nu\text{SiOH}$ band in TMA-SAz-1 (Figure 6B,b) is weaker than that in the Li-SAz-1

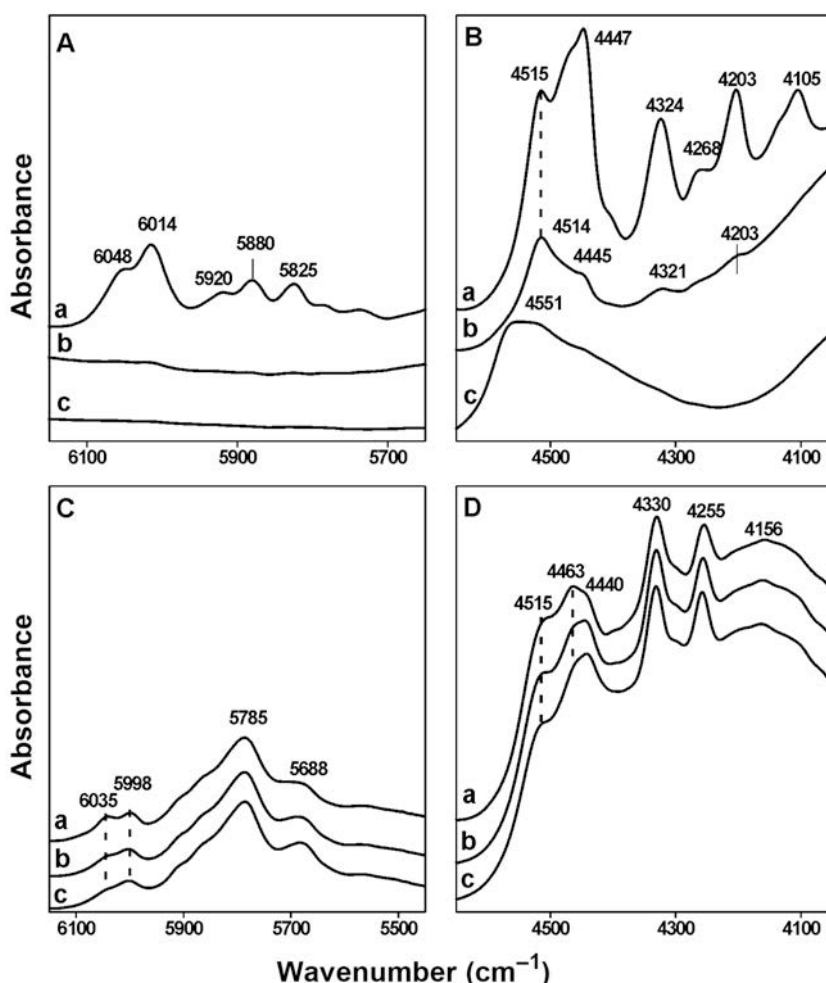


Figure 7. CH overtone and combination regions of TMA-SAz-1 (A, B) and HDTMA-SAz-1 (C, D): untreated (a), treated in 6 M HCl at 80°C for 2 h (b), and 6 h (c).

spectrum (Figure 6A,b) and no clear decrease in the intensity of the 2vOH band is visible in the TMA-SAz-1 spectrum. While the first CH overtone region (Figure 7A,b) showed the disappearance of all bands after 2 h of acid dissolution, the CH combination region (Figure 7B,b) retained some spectral features even after this treatment, indicating it is a more sensitive region in terms of the relics of the CH_3 groups. (Figure 7B,b). Although the $(\nu+\delta)\text{OH}$ band at 4515 cm^{-1} dominates in this region, the presence of the shoulders near 4445 cm^{-1} , 4321 cm^{-1} , and 4203 cm^{-1} confirms that not all the TMA^+ cations were exchanged by protons upon 2 h of treatment. The NIR region distinguishes more sensitively the presence of TMA^+ than does the MIR spectrum (Figure 5) in which the inflection due to δCH_3 vibrations can be only barely resolved in the spectrum of the sample treated for 2 h. The shape of the NIR spectrum of TMA-SAz-1 dissolved for 6 h is similar to that of Li-SAz-1; no bands due to TMA^+ were detected. The intensities of the SiOH overtone (7316 cm^{-1}) and combination (near 4551 cm^{-1}) bands indicate pronounced degradation of the montmorillonite structure (Figure 6B).

Acid dissolution of HDTMA-SAz-1 for 2 or 6 h produced no pronounced changes in its NIR spectra (spectra b and c in Figures 6C, 7C, and 7D). Only an upward shift and a slight decrease in the intensities of the 2vOH and $(\nu+\delta)\text{H}_2\text{O}$ bands in the spectrum of HDTMA-SAz-1 treated for 6 h indicate partial modification of the montmorillonite structure. Only minor changes in the CH overtone and combination regions of HDTMA-SAz-1 were observed after 6 h of treatment (Figures 7C and 7D). An initial doublet at 6035 cm^{-1} and 5998 cm^{-1} , corresponding to $2\nu_{\text{as}}\text{CH}_3\text{-N}$, merged into one broader peak after acid treatment while a shoulder near 5688 cm^{-1} became better resolved. Similarly, the modification of the $(\nu+\delta)\text{CH}_3\text{-N}$ bands at 4463 cm^{-1} and 4440 cm^{-1} can be recognized in the CH combination region of acid-treated HDTMA-SAz-1 (Figure 7D). Apparently the terminal $(\text{CH}_3)_3\text{-N}$ groups are more sensitive to HCl treatment than are the $-\text{CH}_2\text{-C}$ groups.

The NIR spectra of HDTMA-SAz-1 contained, however, one unexpected feature. No SiOH overtone near 7315 cm^{-1} can be distinguished in the spectrum of HDTMA-SAz-1 treated for 6 h, although a small upward shift of the $\nu\text{Si-O}$ band (Figure 5) and changes in the bands at 7060 cm^{-1} and 5246 cm^{-1} (Figure 6) indicate at least some, though minimal, decomposition of the montmorillonite layers. The presence of a SiOH overtone was found to be a very sensitive indicator of the creation of SiOH groups on the clay mineral surface (Pálková *et al.*, 2003). For example, the SiOH overtone was unambiguously identified in the spectrum of acid-treated illite-smectite even when no intensity alteration of the 2vOH overtone and no change in the $\nu\text{Si-O}$ band position were observed (Madejová *et al.*, 2009). The

absence of SiOH overtone in the spectra of acid-treated HDTMA-SAz-1 can only tentatively be explained because no additional results obtained by other methods (*e.g.* NMR spectroscopy or CHN analysis) are available at the moment. Even though the disruption of the octahedral sheets of the HDTMA-SAz-1 after 6 h of treatment in HCl is very limited, some Si-O^- groups should still have been created. The HDTMA^+ released as a result of their partial replacement by H^+ may compensate the unsaturated charge of Si-O^- groups. Consequently, no Si-OH band can be distinguished in the NIR spectrum of acid-treated HDTMA-SAz-1. However, this hypothesis, as was mentioned above, requires verification by other analytical methods.

Both MIR and NIR spectra confirm the different influence of quaternary alkylammonium cations on the acid dissolution of SAz-1 montmorillonite. In comparison with Li^+ , the effect of TMA^+ cations on the dissolution in 6 M HCl is distinguished only after short treatments (*i.e.* 2 h), while after a longer period (*e.g.* 6 h) the extent of dissolution is the same as that of Li-SAz-1. On the other hand, the HDTMA $^+$ cations almost completely prevent decomposition of the montmorillonite layers even after 6 h of acid exposure. The properties of alkylammonium derivates of clay minerals depend on the layer charge of smectite and on the type of alkylammonium cation used (Klapyta *et al.*, 2001; Slade and Gates, 2004; Kooli and Magusin, 2005; Lagaly *et al.*, 2006). Alkylammonium cations with short alkyl chains (TMA^+) are located on the montmorillonite surface as discrete units isolated by uncovered mineral surface that can act as potential access for protons. Due to the high layer charge of SAz-1, a large part of the siloxane surface is covered with TMA^+ and, therefore, the rate of dissolution of TMA-SAz-1 is reduced somewhat in comparison with that of Li-SAz-1. The arrangement of HDTMA $^+$ in the smectite interlayers is different, however. The charged head-groups of HDTMA $^+$ are in direct contact with the siloxane surface while long alkyl chains create a pseudotrimolecular and bimolecular configuration (Lagaly *et al.*, 2006; Slade and Gates, 2007). They also cover the minerals' outer surfaces. Taking into account the high charge of SAz-1 montmorillonite and the size of the HDTMA $^+$, only a limited part of the HDTMA-SAz-1 surface can interact with protons. Decelerated dissolution of HDTMA-SAz-1 reflects a combination of two factors; *i.e.* the poor ability of the organo-clay to swell in aqueous media and limited access of protons to the layers.

CONCLUSIONS

The application of NIR spectroscopy to the study of acid-treated alkylammonium derivatives of SAz-1 montmorillonite has great potential as a characterization tool for clay mineral-organic molecule interactions. Based on the fundamental vibrations observed in the MIR region,

the 2vCH and (v+δ)CH bands have been identified in the NIR spectra of organo-clays. The NIR spectra of acid-treated Li-SAz-1 showed a pronounced decrease in the intensities of structural OH overtone and combination bands, indicating a substantial degradation of the structure. The first SiOH overtone near 7315 cm⁻¹ indicates acidification of the montmorillonite surface and/or creation of a partly protonated silica phase during acid dissolution of the clay mineral. The IR spectra confirm that the dissolution rate of TMA-SAz-1 in 6 M HCl at 80°C is only slightly reduced compared to that of Li-SAz-1, while the long-chain HDTMA⁺ cation protects the montmorillonite layers from acid attack. The IR spectra in both the MIR and NIR regions provide information regarding the different dissolution rates of Li-, TMA-, and HDTMA-SAz-1. Spectra in the NIR region, however, more sensitively reflect the changes in alkylammonium cations during acid treatment. In addition, only the NIR region can monitor the creation of SiOH groups – an important indicator of the surface acidification of montmorillonite. That no SiOH groups were found in the NIR spectrum of HDTMA-SAz-1 dissolved in 6 M HCl at 80°C for 6 h indicates that the HDTMA⁺ completely covers the inner and outer surfaces of montmorillonite and blocks access by protons to the unsaturated Si-O⁻ groups of the SAz-1.

Detailed analysis of the NIR spectra of alkylammonium derivatives of smectites is important for further interpretation of spectra of various organic species adsorbed on clays. The results achieved in this study may also help soil mineralogists using portable field spectrometers utilizing NIR radiation. Acidification of soils, for example, is currently a frequently investigated environmental problem. Accurate interpretations of NIR spectra of acid-treated organo-clays could contribute to more precise analyses of the results obtained directly in the field.

ACKNOWLEDGMENTS

Financial support by the Slovak Grant Agency VEGA (Grant No. 2/6177/06) and Slovak Research and Development Agency (Grant No. APVV-51-050505) is appreciated.

REFERENCES

- Balan, E., Lazzeri, M., Delattre, S., Méheut, M., Refson, K., and Winkler, B. (2007) Anharmonicity of inner-OH stretching modes in hydrous phyllosilicates: assessment from first-principles frozen-phonon calculations. *Physics and Chemistry of Minerals*, **34**, 621–625.
- Bishop, J.L., Pieters, C.M., and Edwards, J.O. (1994) Infrared spectroscopic analyses on the nature of water in montmorillonite. *Clays and Clay Minerals*, **42**, 702–716.
- Bishop, J.L., Murad, E., Lane, M.D., and Mancinelli, R.L. (2004) Multiple techniques for mineral identification on Mars: a study of hydrothermal rocks as potential analogues for astrobiology sites on Mars. *Icarus*, **169**, 311–323.
- Bishop, J.L., Noe Dobrea, E.Z., McKeown, N.K., Parente, M., Ehlmann, B.L., Michalski, J.R., Milliken, R.E., Poulet, F., Swayze, G.A., Mustard, J.F., Murchie, S.L., and Bibring, J.-P. (2008a) Phyllosilicate diversity and past aqueous activity revealed at Mawrth Vallis, Mars. *Science*, **321**, 830–833.
- Bishop, J.L., Lane, M.D., Dyar, M.D., and Brown, A.J. (2008b) Reflectance and emission spectroscopy study of four groups of phyllosilicates: smectites, kaolinite-serpentines, chlorites and micas. *Clay Minerals*, **43**, 35–54.
- Bokobza, L. (1998) Near infrared spectroscopy. *Journal of Near Infrared Spectroscopy*, **6**, 3–17.
- Boyd, S.A., Mortland, M.M., and Chiou, C.T. (1988) Sorption characteristics of organic compounds on hexadecyltrimethylammonium-smectite. *Soil Science Society of America Journal*, **2**, 652–657.
- Breen, C., Watson, R., Madejová, J., Komadel, P., and Klapýta, Z. (1997) Acid-activated organo-clays: Preparation, characterization and catalytic activity of acid-treated tetraalkylammonium-exchanged smectites. *Langmuir*, **13**, 6473–6479.
- Breen, C. and Watson, R. (1998) Acid-activated organo-clays: preparation, characterisation and catalytic activity of polycation-treated bentonites. *Applied Clay Science*, **12**, 479.
- Dill, H.G., Kaufhold, S., Khishigsuren, S., and Bulgamaa, J. (2005) Discovery and origin of a Palaeogene smectite-bearing clay deposit in the SE Gobi (Mongolia). *Clay Minerals*, **40**, 351–367.
- Farmer, V.C. (1974) The layer silicates Pp. 331–363 in: *Infrared Spectra of Minerals* (V.C. Farmer, editor). Mineralogical Society, London.
- Frost, R.L., Kloporgge, J.T., and Ding, Z. (2002) Near-infrared spectroscopic study of nontronites and ferruginous smectite. *Spectrochimica Acta A*, **58**, 1657–1668.
- Frost, R.L., Zhou, Q., He, H.P., and Xi, Y.F. (2008) An infrared study of adsorption of para-nitrophenol on mono-, di- and tri-alkyl surfactant intercalated organo-clays. *Spectrochimica Acta A*, **69**, 239–244.
- Gates, W.P. (2005) Infrared spectroscopy and the chemistry of dioctahedral smectites. Pp. 126–168 in: *The Application of Vibrational Spectroscopy to Clay minerals and Layered Double Hydroxides* (J.T. Kloporgge, editor). CMS Workshop Lectures 13, The Clay Minerals Society, Aurora, Colorado, USA.
- Gates, W.P., Slade, P., Manceau, A., and Lanson, B. (2002) Site occupancies by iron in nontronites. *Clays and Clay Minerals*, **50**, 223–239.
- Gionis, V., Kacandes, G.H., Kastritis, I.D., and Chryssikos, G.D. (2007) Combined near-infrared and X-ray diffraction investigation of the octahedral sheet composition of palygorskite. *Clays and Clay Minerals*, **55**, 543–553.
- Hunt, G.R. and Salisbury, J.W. (1970) Visible and near infrared spectra of minerals and rocks: VI. Silicate minerals. *Modern Geology*, **1**, 283–300.
- Klapýta, Z., Fujita, T., and Iyi, N. (2001) Adsorption of dodecyl- and octadecyltrimethylammonium ions on smectite and synthetic micas. *Applied Clay Science*, **19**, 5–10.
- Komadel, P. and Madejová, J. (2006) Acid activation of clay minerals. Pp. 263–287 in: *Handbook of Clay Science* (F. Bergaya, B.K.G. Theng, and G. Lagaly, editors). Developments in Clay Science, Vol. 1. Elsevier Ltd., Amsterdam.
- Komadel, P., Madejová, J., Janek, M., Gates, W.P., Kirkpatrick, R.J., and Stucki, J.W. (1996) Dissolution of hectorite in inorganic acids. *Clays and Clay Minerals*, **44**, 228–236.
- Kooli, F. and Magusin, C.M.M. (2005) Adsorption of cetyltrimethylammonium ions on an acid-activated smectite and their thermal stability. *Clay Minerals*, **40**, 233–243.
- Lagaly, G., Ogawa, M., and Dékány, I. (2006) Clay mineral organic interactions. Pp. 309–377 in: *Handbook of Clay Science* (F. Bergaya, B.K.G. Theng, and G. Lagaly, editors).

- Developments in Clay Science, Vol. 1. Elsevier Ltd., Amsterdam.
- Madejová, J. (2005) Studies of reduced-charge smectites by near infrared spectroscopy. Pp. 169–202 in: *The Application of Vibrational Spectroscopy to Clay Minerals and Layered Double Hydroxides* (J.T. Kloprogge, editor). CMS Workshop Lectures 13, The Clay Minerals Society, Aurora, Colorado, USA.
- Madejová, J. and Komadel, P. (2001) Baseline studies of the Clay Minerals Society Source Clays: Infrared methods. *Clays and Clay Minerals*, **49**, 410–432.
- Madejová, J., Bujdák, J., Petit S., and Komadel, P. (2000) Effects of chemical composition and temperature of heating on the infrared spectra of Li-saturated dioctahedral smectites: (II) Near-infrared region. *Clay Minerals*, **35**, 753–761.
- Madejová, J., Andrejkovičová, S., Bujdák, J., Čeklovský, A., Hrachová, J., Valúchová, J., and Komadel, P. (2007) Characterization of products obtained by acid leaching of Fe-bentonite. *Clay Minerals*, **42**, 527–540.
- Madejová, J., Penetrák, M., Pálková, H., and Komadel, P. (2009) Near-infrared spectroscopy: a powerful tool in studies of acid-treated clay minerals. *Vibrational Spectroscopy*, **49**, 211–218.
- Malley, D.F., Yesmin, L., and Eilers, R.G. (2002) Rapid analysis of hog manure and manure-amended soils using near-infrared spectroscopy. *Soil Science Society of America Journal*, **66**, 1677–1686.
- Moronta, A., Ferrer, V., Quero, J., Arteaga, G., and Choren, E. (2002) Influence of preparation method on the catalytic properties of acid-activated tetramethylammonium-exchanged clays. *Applied Catalysis A: General*, **230**, 127–135.
- Önal, M. and Sankaya, Y. (2008) Some physicochemical properties of methylammonium and ethylenediammonium smectites. *Colloids Surfaces A: Physicochemical Engineering Aspects*, **312**, 56–61.
- Pálková, H., Madejová, J., and Righi, D. (2003) Acid dissolution of reduced-charge Li- and Ni-montmorillonites. *Clays and Clay Minerals*, **51**, 133–142.
- Petit, S. (2005) Crystal-chemistry of talcs: a NIR and MIR spectroscopic approach. Pp. 41–64 in: *The Application of Vibrational Spectroscopy to Clay Minerals and Layered Double Hydroxides* (J.T. Kloprogge, editor). CMS Workshop Lectures, 13. The Clay Minerals Society, Aurora, Colorado, USA.
- Petit, S., Madejová, J., Decarreau, A., and Martin F. (1999) Characterization of octahedral substitutions in kaolinites using near infrared spectroscopy. *Clays and Clay Minerals*, **47**, 103–108.
- Petit, S., Caillaud, J., Righi, D., Madejová, J., Elsass, F., and Köster, H.M. (2002) Characterization and crystal chemistry of a Fe-rich montmorillonite. *Clay Minerals*, **37**, 283–297.
- Petit, S., Decarreau, A., Martin, F. and Buchet, R. (2004) Refined relationship between the position of the fundamental OH stretching and the first overtones for clays. *Physics and Chemistry of Minerals*, **31**, 585–592.
- Prüfer, H. and Mamma, D. (1995) Near-infrared online analysis of motor octane number in gasoline with an acoustooptic tunable transmission spectrophotometer. *Analysis*, **23**, M14–M18.
- Slade, P.G. and Gates, W.P. (2004) The swelling of HDTMA smectites as influenced by their preparation and layer charge. *Applied Clay Science*, **25**, 93–101.
- Slade, P.G. and Gates, W.P. (2007) HDTMA in the interlayers of high-charged Llano vermiculite. *Clays and Clay Minerals*, **55**, 131–139.
- Stevens, J.J. and Anderson, S.J. (1996) An FTIR study of water sorption on TMA- and TMPA-montmorillonites. *Clays and Clay Minerals*, **44**, 142–150.
- Theng, B.K.G. (1974) *The Chemistry of Clay-Organic Reactions*. Adam Hilger, London.
- Tkáč, I., Komadel, P., and Müller, D. (1994) Acid-treated montmorillonites – a study by ^{29}Si and ^{27}Al MAS-NMR. *Clay Minerals*, **29**, 11–19.
- Williams, P. and Norris, K. (1987) *Near-infrared Technology in the Agricultural and Food Industries*. American Association of Cereal Chemists, St. Paul, Minnesota, USA.
- Worckman, J. and Weyer, L. (2008) *Practical Guide to Interpretive Near-infrared Spectroscopy*. Taylor & Francis Group, Boca Raton, Florida, USA.
- Yariv, S. (2001) IR spectroscopy and Thermo-IR spectroscopy in the study of the fine structure of organo-clay complexes. Pp. 345–462 in: *Organoclay Complexes and Interactions* (S. Yariv and H. Cross, editors). Marcel Dekker, Inc, New York.
- Yariv, S. and Cross, H. (2001) *Organoclay Complexes and Interactions*. (S. Yariv and H. Cross, editors). Marcel Dekker, Inc. New York.
- Zeegers-Huyskens, T. and Bator, G. (1996) Fourier transform infrared and Fourier transform Raman investigation of alkylammonium hexachloroantimonates. *Vibrational Spectroscopy*, **13**, 41–49.
- Zhou, Q., Xi, Y., He, H., and Frost, R.L. (2008) Application of near infrared spectroscopy for the determination of adsorbed p-nitrophenol on HDTMA organo-clay – implications for the removal of organic pollutants from water. *Spectrochimica Acta A*, **69**, 835–841.
- Zhu, J., He, H., Zhu, L., Wen, X., and Deng, F. (2005) Characterization of organic phases in the interlayer of montmorillonite using FTIR and C-13 NMR. *Journal of Colloid and Interface Science*, **286**, 239–244.

(Received 3 November 2008; revised 10 March 2009;
Ms. 0225; A.E. W.P. Gates)